The Cryosphere Discuss., https://doi.org/10.5194/tc-2018-142
Manuscript under review for journal The Cryosphere
Discussion started: 7 August 2018

The Cryosphere Discussions
Open Access
EGU

Anomalous acceleration of mass loss in the Greenland ice sheet drainage basins and its contribution to the sea level fingerprints during 2010－2012

Linsong Wang[1,2], Liangjing Zhang[2], Chao Chen[1], Maik Thomas[2,3], and Mikhail K. Kaban[2]

[1] Hubei Subsurface Multi-scale Imaging Key Laboratory, Institute of Geophysics and Geomatics, China University of Geosciences, Wuhan 430074, China

[2] Helmholtz Centre Potsdam, GFZ German Research Centre for Geosciences, Telegrafenberg, Potsdam 14473, Germany

[3] Institute of Meteorology, Freie Universität Berlin, Berlin, Germany

Correspondence: Linsong Wang (wanglinsong@cug.edu.cn)

Abstract. The sea level rise contributed from ice sheet melting has been accelerating due to global warming. Continuous melting of the Greenland ice sheet (GrIS) is a major contributor to sea level rise, which impacts directly on the surface mass balance and the instantaneous elastic response of the solid Earth. To study the sea level fingerprints (SLF) caused by the anomalous acceleration of the mass loss in GrIS can help us to understand drivers of sea level changes due to global warming and the frequently abnormal climate events. In this study, we focus on the anomalous acceleration of the mass loss in GrIS at the drainage basins from 2010 to 2012 and on its contributions to SLF and relative sea level (RSL) changes based on self-attraction and loading effects. Using GRACE monthly gravity fields and surface mass balance (SMB) data spanning 13 years between 2003 and 2015, the spatial and temporal distribution of the ice sheet balance in Greenland is estimated by mascons fitting based on six extended drainage basins and matrix scaling factors. Then the SLF spatial variations are computed by solving the sea level equation. Our results indicate that the total ice sheet mass loss is contributed from few regions only in Greenland,

The Cryosphere Discuss., https://doi.org/10.5194/tc-2018-142
Manuscript under review for journal The Cryosphere
Discussion started: 7 August 2018

i.e., from the northwest, central west, southwestern and southeastern parts. Especially along the north-west coast and the south-east coast, ice was melting significantly during 2010–2012. The total mass loss rates during 2003–2015 are −288±7 Gt/yr and −275±1 Gt/yr as derived from scaled GRACE data and SMB respectively; and the magnitude of the trend increased to −456±30 Gt/yr and to −464±38 Gt/yr correspondingly over the period 2010–2012. The residuals obtained by GRACE after removing SMB show a good agreement with the surface elevation change rates derived from pervious ICESat results, which reflect a contribution from glacial dynamics to the total ice mass changes. Melting of GrIS results in decreased RSL in Scandinavia and North Europe, up to about −0.6 cm/yr. The far-field peak increase is less dependent on the precise pattern of self-attraction and loading; and the average global RSL was raised by 0.07 cm/yr only. Greenland contributes about 31% of the total terrestrial water storage transferring to the sea level rise from 2003 to 2015. We also found that variations of the GrIS contribution to sea level have an opposite V shape (i.e., from rising to falling) during 2010–2012, while a clear global mean sea level drop also took place (i.e., from falling to rising).

Key words. GRACE; SMB; Greenland ice sheet; anomaly melting; sea level fingerprints

The Cryosphere Discuss., https://doi.org/10.5194/tc-2018-142
Manuscript under review for journal The Cryosphere
Discussion started: 7 August 2018

1 Introduction

The sea level rise due to melting of ice sheets, glaciers and ice caps has been accelerating in consequence of global warming. The mass change of polar ice sheets is a major global concern, especially due to its direct impact to global sea level rise (Forsberg et al., 2017). Estimation of the global ice balance has been obviously improved in recent years based on available satellite observations, model simulations and the development of data processing technologies, e.g., using the Gravity Recovery and Climate Experiment (GRACE) (Rodell et al., 2009; Jacob et al., 2012; Velicogna et al., 2014) and the Ice, Cloud, and land Elevation Satellite (ICESat) (Zwally et al., 2011; Shepherd et al., 2012; Gardner et al., 2013). In the last decade, most studies have confirmed that significant mass loss takes place in the ice sheets of Greenland and Antarctica, which corresponds to approximately 7 m and 57 m of the sea level rise respectively when the mass is completely melted (Bamber et al., 2001; Lythe et al., 2001). Therefore, there is a high demand to monitor the trend in mass balance changes over Greenland and Antarctica to better understand global climate change and associated sea level rise.

Due to global warming, frequency and intensity of extreme weather events (i.e., snowstorms, cold currents, torrential rains, heat waves, etc.) are increasing globally. Since the early 1990s, satellite data show that the global mean sea level has been rising by about 3 mm/yr. Numerous scientific papers on ice sheet changes and their contribution to sea level rise have been published based on satellite observations over the last decade, but we still need to focus on the continental ice mass balance caused by abnormal climate fluctuations in a short term period. A solitary wave disturbance of global mean sea level has happened during 2010–2012, when the sea level decreased by 5 mm from the beginning of 2010 to mid 2011 and then rose by nearly 20 mm until the end of 2012 (NASA: SEA LEVEL CHANGE Observations from Space). This occurred along with a La Niña phase of the El Niño–Southern Oscillation (ENSO). Previous studies have shown that the change in the sea level

The Cryosphere Discuss., https://doi.org/10.5194/tc-2018-142
Manuscript under review for journal The Cryosphere
Discussion started: 7 August 2018

77 during La Niña is related to water temporarily moved from the oceans to the land,
78 when precipitation increased over Australia, northern South America, and Southeast
79 Asia, while it decreased over the oceans. Increased precipitation in Australia is proven
80 to be the dominant contributor to the global total sea level change in 2011 (Boening et
81 al., 2012; Fasullo et al., 2013).
82

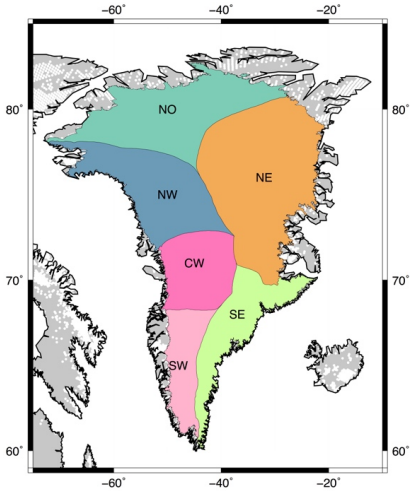

Figure 1. Greenland drainage basins. NO: north; NE: northeast; SE: southeast; SW: southwest; CW: central west and NW: northwest according to Rignot Basins from IMBIE 2016 (Rignot et al., 2011). White dots show ice caps in Greenland and surrounding areas.

83

84 It is well known that the Greenland ice sheet (GrIS) plays an important role in Earth
85 system dynamics, which not only affects sea level but also contributes to the elastic
86 response of the solid Earth. Here, we present detailed mass balance results for the
87 GrIS drainage basins by estimating the anomalous acceleration of the mass loss and
88 its contributions to sea level fingerprints (SLF). Figure 1 shows Greenland ice
89 drainage units, named Rignot Basins from IMBIE 2016 (Ice Sheet Mass Balance
90 Intercomparison Experiment), which are based on historical usage (Rignot et al.,
91 2011). The GrIS is divided into six regions based on the glacier regime. Central west

The Cryosphere Discuss., https://doi.org/10.5194/tc-2018-142
Manuscript under review for journal The Cryosphere
Discussion started: 7 August 2018

and northwest have a clear basin boundary near Rinks. Central west to southwest mark the transition from tidewater to land-terminating. Southeast vs northeast chiefly represents a transition in the surface mass balance (SMB) with a well-defined divide inland. We use GRACE monthly gravity fields and the monthly cumulative SMB from the Regional Atmospheric Climate Model (RACMO) to estimate the spatial distribution of the ice mass balance. The time series of mass changes were estimated by a mascon fitting method described by Jacob et al. (2012). The relative sea level (RSL) spatial variations were computed by solving the sea level equation with self-attraction and loading effects. Based on the above results, we further discuss the sensitivity kernels and rescaled GrIS time series due to the limitation of exact-defined basin mask and GRACE resolution; we also analyze spatial variations of the abnormal melting in glaciers, near-surface air temperature over Greenland and contributions of GrIS to sea level changes.

2 Data and methods

2.1 GRACE

The GRACE mission design makes it particularly useful for surface mass variations studies. GRACE was jointly launched by NASA and the German Aerospace Center (DLR) in March 2002 (Tapley et al. 2004). The Level-2 gravity products provide complete sets of spherical harmonic (Stokes) coefficients, typically up to the maximum degree/order l_{max}=120, averaged over monthly intervals. Detection of mass change using GRACE data becomes a widely used tool for estimation of the ice sheet mass balance due to the operational difficulties of other measurements over large areas. However, interpretation of GRACE data is complicated by the intrinsic mixing of gravity signals. Glacial isostatic adjustment (GIA) can be corrected by modeling the lithospheric response to loading changes (Velicogna and Wahr, 2006) while other mass change contributions (e.g., terrestrial water storage) are smaller on ice sheets compared to other areas.

The Cryosphere Discuss., https://doi.org/10.5194/tc-2018-142
Manuscript under review for journal The Cryosphere
Discussion started: 7 August 2018

120 In this study, we use monthly sets of spherical harmonics from the GRACE Release
121 05 (RL05) gravity field solutions generated by the Center for Space Research (CSR)
122 at the University of Texas, spanning January 2003 to December 2015. Each monthly
123 GRACE field consists of a set of Stokes coefficients, C_{lm} and S_{lm}, up to degree and
124 order (l and m) of 60. We replaced the GRACE C_{20} coefficients with the results
125 inferred from satellite laser ranging (Cheng et al. 2013), and include degree-one
126 coefficients as calculated by Swenson et al. (2008). The Stokes coefficients from A et
127 al. (2013) are used to remove the GIA effect.

128 **2.2 SMB**

129 In several studies RACMO and the Firn Densification Model (FDM) have been
130 applied for Greenland using different models at different resolutions and with various
131 forcing at the boundaries. To further compare and validate the GRACE-derived mass
132 changes, we use monthly SMB fields to simulate GrIS mass balance from RACMO
133 version 2.3 (RACMO2.3), which are provided on a grid of about 40 vertical layers
134 and a horizontal resolution of ~11×11 km^2 for the period January 1958–December
135 2015 (Noël et al., 2015). Then we analyze the spatial and temporal patterns of glacial
136 dynamics components combining GRACE and SMB data.

137

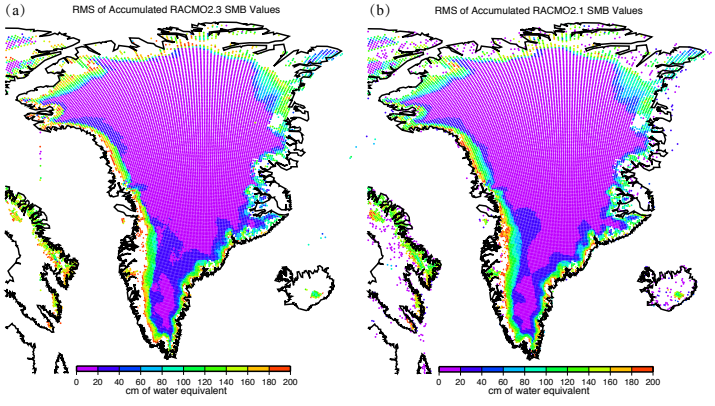

Figure 2. Root mean square errors of accumulated SMB values in RACMO2.3 (a) and RACMO2.1 (b) during 1960 to 2011.

The Cryosphere Discuss., https://doi.org/10.5194/tc-2018-142
Manuscript under review for journal The Cryosphere
Discussion started: 7 August 2018

The latest version of RACMO2.3 has been specifically developed to simulate SMB of glaciated regions as an updated version of RACMO2.1 (Ettema et al., 2009; Van Angelen et al., 2014). Figure 2 shows root mean square errors of accumulated SMB values in two versions for the period 1960 to 2011. Both models consist of 312 (latitude) × 306 (longitude) grid cells and include Iceland, the Svalbard archipelago and the Canadian Arctic. Overall, there is no significant difference in the cumulative root mean square (1960–2011) between the two versions of the model, but RACMO2.3 shows larger fluctuations at the boundary of GrIS. This is mainly due to the fact that RACMO2.3 is forced at the lateral boundaries by the 40-year European Centre for Medium-Range Weather Forecasts (ECMWF) Reanalysis (ERA-40) for the period January 1958–December 1979 and the ECMWF Interim Reanalysis (ERA-Interim) afterwards (van den Broeke et al., 2016).

In this study, we first used the GrIS mask as prescribed in RACMO2.3 to remove effects of the ice caps from entire SMB in Greenland and integrated them over time to get accumulated SMB values. Because SMB represents the sum of mass fluxes inside and away from ice sheets, the mass balance of the grounded ice sheet is governed by the difference between SMB and the solid ice discharge across the grounding line. Thus, the ice discharge must be subtracted from the accumulated SMB (SMB minus ice discharge) to be compared with GRACE (van den Broeke et al., 2016). After removing the temporal average of the accumulation rates at each point, we convert SMB data to the spectral domain and truncate them to degree 60, i.e., the limit of the GRACE data.

2.3 Other datasets

Initially, we employed the Noah land hydrology model (version 2) in the Global Land Data Assimilation System (GLDAS-2) to remove continental water mass contributions, but we found that there is a large error in the results. The global GLDAS/Noah, which possesses monthly intervals with a spatial resolution of 1.0 degree, provides a total amount of the water stored in all layers, snow, and canopy, but

166 does not include the groundwater and water storage changes in rivers or lakes (Rodell
167 et al., 2004). It also excludes the water storage estimates from the GrIS and
168 permafrost areas (Liu et al., 2016). Likely, the abnormally large snow values obtained
169 for Greenland are a result of unreliable forcing data. We simulated mass changes from
170 the soil moisture component and found that the soil moisture from GLDAS is
171 dominated by the annual cycle and the annual amplitudes are much smaller than the
172 GrIS change. Finally, we ignored the terrestrial water storage (e.g., mainly presented
173 as seasonal changes, no obvious long-term trend) impacts on the mass change in
174 Greenland and assumed that the mass balance revealed by GRACE data is mainly due
175 to ice sheet changes.
176 A previous study based on satellite-derived ice-surface temperature has confirmed a
177 positive trend of the near surface temperature of GrIS and two major melt events from
178 2000 to present (Hall et al., 2013). Therefore, we chose the temperature data from the
179 GLDAS/Noah model, which integrates the latest NASA remote sensing products (e.g.,
180 moderate-resolution imaging spectro-radiometer, MODIS). We investigated whether
181 there was clear correlation in spatial distribution of the GLDAS/Noah forcing data
182 (i.e., temperature) and the GrIS variations spanning from 2003 to 2015.
183 On climate timescales, the global mean sea level rise is mainly caused by increasing
184 volume of the global ocean in consequences of thermal expansion) and increasing
185 ocean mass due to water masses from land (i.e., GRACE-derived barystatic sea level
186 rise caused by loss of ice and reduction of liquid water storage on land). Reliable time
187 series of global mean sea level based on satellite altimetry (TOPEX/Poseidon, Jason-1
188 and OSTM/Jason-2) are available since September 1992 (the global mean sea level
189 data was downloaded from NASA, available at:
190 https://sealevel.nasa.gov/understanding-sea-level/key-indicators/global-mean-sea-leve
191 l). All biases and cross-calibrations have been applied to the data, therefore sea
192 surface height anomalies derived from various altimetry missions are expected to be
193 consistent. The data have been presented as changes relative to January 1, 1993

The Cryosphere Discuss., https://doi.org/10.5194/tc-2018-142
Manuscript under review for journal The Cryosphere
Discussion started: 7 August 2018

194 averaged over 2-months intervals. The GIA correction has been applied to the data
195 (Beckley et al., 2017). To estimate steric sea level anomalies, we used time series of
196 3-month total steric sea level anomaly data, which is a contribution of the changes in
197 the global ocean heat storage for the 0–700 m and 0–2000 m layers (the total steric
198 sea level anomaly data was downloaded from NOAA, available at:
199 https://www.nodc.noaa.gov/OC5/3M_HEAT_CONTENT/basin_fsl_data.html).

200 **2.4 Spatial Averaging and scaling factor methods**

201 Observations of mass variability are, in particular, useful for estimates of changes of
202 continental water storage. These water storage changes are generally addressed by
203 constructing specific averaging functions optimized for each region (Swenson and
204 Wahr, 2002). Note that the averaging kernel method implies a Gaussian averaging
205 function at each point, and sums those averaging functions expressed as the finite
206 number of harmonic degrees in the GRACE solution (e.g. $l_{max} = 60$ for CSR solutions).
207 Thus, the optimal averaging kernel technique provides an estimate of the total mass
208 change of the region but does not give accurate estimates of sub-regions, such as
209 those in Figure 1, due to the spatial resolution of the GRACE data. Therefore, the
210 effect of mass changes is spread up to several hundred kilometers outside the region.
211

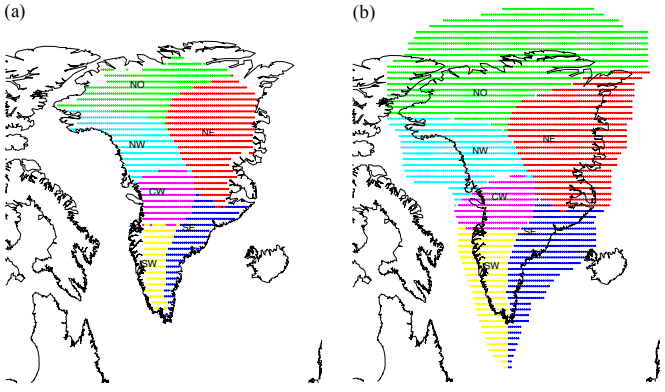

Figure 3. Mascons for the GrIS drainage basins (a). Each colored region represents a single mascon. (b) similar to Figure 3a but for the extended mask of six mascons.

The Cryosphere Discuss., https://doi.org/10.5194/tc-2018-142
Manuscript under review for journal The Cryosphere
Discussion started: 7 August 2018

In this case, we applied an approximation mascon fitting method to GRACE and SMB data to perform a comparison at the regional level. This fitting method is based on the least squares mascon approach to calculate the averaged time series for each region (Jacob et al., 2012; Sutterley et al., 2014). To evaluate the spatial differences in the melting of GrIS at a regional scale, we divided the ice sheet into six extended mascons as shown in Figure 3, and each mascon was composed of small blocks defined on a 0.5-degree grid; a unit mass equal to 1 cm of water was distributed uniformly over the block (Farrell 1972). We applied a 150-km Gaussian smoothing function on the Stokes coefficients for the GRACE (GIA corrected), SMB and all mascon coefficients.

We simultaneously fit the extended mascon Stokes coefficients, in which GrIS is represented by a single basin, to monthly GRACE coefficients (after post-processing described in section 2.1) to obtain estimates of monthly mass variability for each mascon. The corresponding result in terms of time series of entire GrIS is shown in Figure 4. When using extended mascons, the mass loss is assumed to be uniformly distributed over mascons, which is not the case everywhere (e.g., because there is no or relatively small mass change over the oceans). Thus, it is necessary to identify a realistic scaling factor. Assuming that there is a 1 cm uniform layer over exact and extended GrIS, the total mass is 17.495 Gt and 39.303 Gt, respectively. We used the exact Greenland mascon as the input to fit the extended mascon to the input signal. In this way, the 0.537 cm uniform mass is obtained over the extended GrIS, which is equivalent to a 46% reduction in ice thickness of the input mass, which is in good agreement with previous studies based on averaging functions extended outside Greenland (Velicogna and Wahr, 2006). The final scaling factor of the mass inferred is (39.303/17.495) ×0.537=1.206. Therefore, the mass changes estimated with the extended mascon are larger by a factor of 1.206 when degree and order of Stokes coefficients are limited to 60 (Figure 4).

The Cryosphere Discuss., https://doi.org/10.5194/tc-2018-142
Manuscript under review for journal The Cryosphere
Discussion started: 7 August 2018

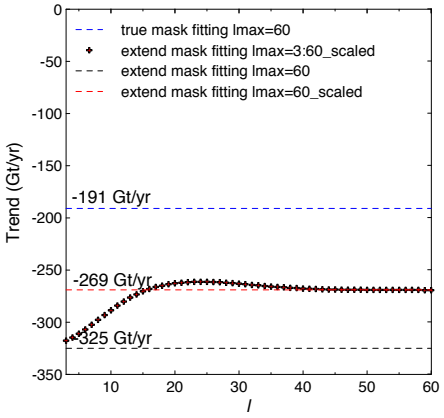

Figure 4. Time series for the entire GrIS from the exact and extended mascons to fit monthly GRACE coefficients. Red crosses are scaled extended mascon fitting results due to change of the scale factor for different degree (*l*).

We take into account the fact that the effect of each mascon could smear into the neighboring ones. Supposing that the mass spread is uniform over the truly $mascon_i$, we computed the Stokes coefficients from the input mass, and then fit extended $mascon_k$ to the set of Stokes coefficients. Basing on the scaling method described above, those values can be used to construct a ratio matrix *A(k,j)*, which is the contribution of those Stokes coefficients to the result for $mascon_k$. Time series for selected regions were calculated using the corresponding mascons to fit GRACE Stokes coefficients. If *M(j)* are the true mascon values, and *N(k)* are the values that we get from the mascon fitting, then the linear observation equations is $N(k) = \sum_{j=1}^{6} A(k,j) \times M(j)$. Therefore, the true mascon values may be solved in a generalized inversion by $M(j) = A^{-1}(k,j) \times N$. This method not only estimates the total mass change but also provides time series for each sub-area after the leakage correction. However, it is worth noting that the extended mascon increases the weight of the boundary in the sensitivity kernels and also causes external leakage in the fitting results, e.g., mass change from the external glaciers, ice caps and eustatic sea level.

The Cryosphere Discuss., https://doi.org/10.5194/tc-2018-142
Manuscript under review for journal The Cryosphere
Discussion started: 7 August 2018

256 The sensitivity kernels and leakage effects are explained in details in Section 4.1.

257 **2.5 Sea level fingerprint**

258 The global SLF reflects the redistribution of ocean-land masses driven by climate
259 change; and these load changes cause the elastic structural response of the crust and
260 affect the viscosity and strength of the lower mantle of the Earth (Peltier and Andrews,
261 1976). RSL changes, for instance, caused by GIA span over a time scale of 1 to 10000
262 years. However, for shorter time scales (1 to 100 years), melting of ice sheets, glaciers
263 and ice caps directly leads to increase of ocean volume and causes instantaneous
264 elastic deformation of the solid Earth. RSL is the height of the sea surface relative to
265 the sea floor, which is defined as the difference between the geoid and the crust. The
266 RSL solution is often referred as the fingerprint of terrestrial mass changes.
267 In this study we use scaled monthly (1 degree × 1 degree) mass change grids of GrIS
268 as input to solve the self-consistent sea level equation (Farrell and Clark, 1976; Milne
269 et al., 1999) and calculate regional SLF due to self-attraction and loading effects
270 (Tamisiea, 2010) of mass changes on Greenland. We use the load Love numbers given
271 by Jentzsch (1997), which were calculated using the 1-D PREM elastic Earth model
272 (Dziewonski and Anderson, 1981). We also consider the Earth rotation feedback but
273 neglect changes in the coastline and effects of atmospheric and non-tidal ocean
274 loading for short-term sea level variations during 2003 to 2015.
275

276 **3 Results**

277 **3.1 Spatial GrIS variability**

278 The spatial pattern of long-term mass trend, shown in Figure 5, was obtained from the
279 monthly GRACE mass solutions for Greenland from 2003 to 2009 (a), 2010 to 2012
280 (b), 2013 to 2015 (c) and 2003 to 2015 (d). A clear negative trend was identified
281 across the entire ice sheet except in high altitude areas (>2000 m) in the central part.
282 During 2003–2015, the mass loss increased in northwest, central west, south west and
283 southeast, especially along the north-west coast and the south-east coast. In the north

The Cryosphere Discuss., https://doi.org/10.5194/tc-2018-142
Manuscript under review for journal The Cryosphere
Discussion started: 7 August 2018

284 and northeast, the mass melted relatively slowly compared to the other four areas. The
285 ice mass loss increased in 2010–2012 and 2013–2015 relative to 2003–2009.
286 Especially important is that during 2010–2012 a large mass loss is revealed in the
287 entire southern and western regions of Greenland (Figure 5b), which reflects a major
288 melting event that took place in this period. For example, the anomalous warm
289 summer and declined albedos associated with the north Atlantic oscillation led to
290 increased temperatures over Greenland in 2010 (Box et al., 2012). Consequently, the
291 extreme melt event took place over almost the entire surface of the GrIS in 2012
292 (Nghiem et al. 2012).
293

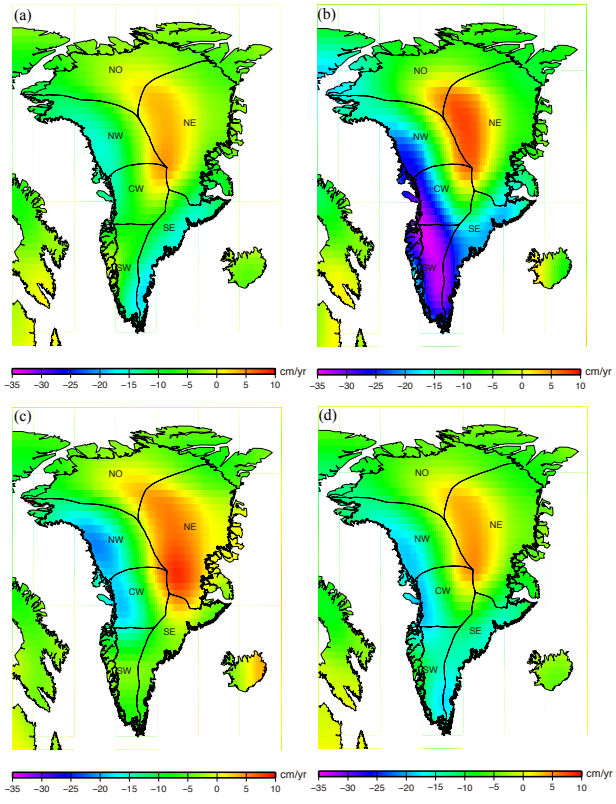

Figure 5. GRACE-derived linear trends of GrIS ice mass balance in 2003–2009 (a), 2010–2012 (b), 2013–2015 (c) and 2003–2015 (d).

294

The Cryosphere Discuss., https://doi.org/10.5194/tc-2018-142
Manuscript under review for journal The Cryosphere
Discussion started: 7 August 2018

295 Figure 6 shows spatial patterns of ice mass changes from SMB data. In 2003–2015,
296 the SMB results indicate that ice mass loss and thinning was concentrated in the entire
297 coastline as well as in western and southeast basins of Greenland. In 2010–2012, mass
298 loss and thinning were stronger in the northwest, central west, south west and
299 southeast; and this spatial and temporal distribution is very consistent with the
300 GRACE-derived mass loss. However, the trend magnitude of SMB is smaller than of
301 the GRACE results. Additionally, we shall keep in mind that the GRACE-derived
302 results reflect mass changes of both SMB and ice discharge, e.g., beginning at 1995,
303 SMB decreased while ice discharge increased, due to acceleration of the ice melting
304 in several large outlet glaciers in the southeast and northwest, which leading to a
305 quasi-persistent negative mass balance (van den Broeke et al., 2016). Moreover,
306 because of large runoff and surface mass fluxes (i.e., meltwater and snowfalls) at the
307 boundary of the GrIS, the current horizontal resolution of RACMO2.3 (11 km) is
308 insufficient to resolve individual, low-lying outlet glaciers of the GrIS (Noël et al.,
309 2016), which leads to potentially large errors and uncertainties in accumulated SMB
310 values (Figure 2).
311

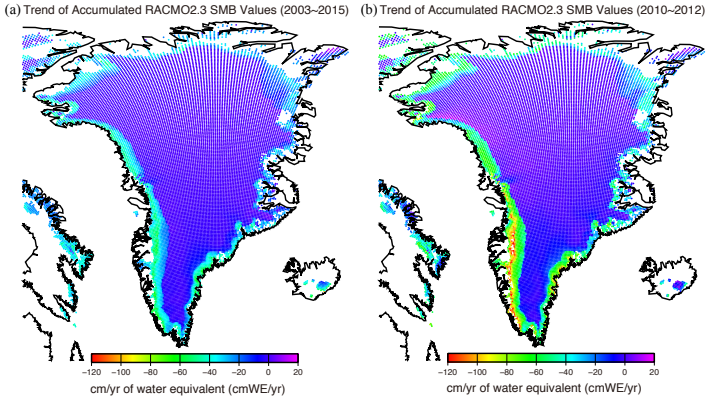

Figure 6. SMB trend in millimeter water equivalent per year or (mmWE/yr) obtained from the RACMO2.3 monthly SMB fields. (a) 2003 to 2015 and (b) 2010 to 2012.

The Cryosphere Discuss., https://doi.org/10.5194/tc-2018-142
Manuscript under review for journal The Cryosphere
Discussion started: 7 August 2018

312 **3.2 Time series of mass change**

313 In order to obtain time series of GrIS mass changes we applied the basin estimation
314 and scaling method described in Section 2 (Figure 7). Representing GrIS by single
315 and extended mascons, we found that the scaled trend rate (–269 Gt/yr when l_{max}=60
316 shown in Figure 4) from 2003 to 2015 in the whole GrIS region is in good agreement
317 with that reported by –270 Gt/yr during 2003–2012 (Schrama et al., 2014) and –270
318 Gt/yr during 2003–2014 (van den Broeke et al., 2016). When the GrIS is represented
319 by six extended basins, the results also show a continuous decrease both before and
320 after scaling (top and bottom left in Figure 7) from 2003 to 2015; since 2010, the rate
321 of this decrease suddenly accelerated towards the end of 2012. The rate of the mass
322 loss obtained by scaled GRACE and SMB is also similar, –288±7 Gt/yr in GRACE
323 and –275±1 Gt/yr in SMB from 2003 to 2015. The magnitude of the trend increased
324 significantly over the period 2010–2012, about –456±30 Gt/yr in GRACE and –
325 464±38 Gt/yr in SMB. The errors here represent fitting uncertainties, while the real
326 uncertainties are mainly due to the GIA correction, leakage of signal from outside ice
327 sheet, and GRACE measurement errors. Those effects in the trends were estimated to
328 be 20 Gt/yr in both time series (Van den Broeke et al., 2009). Our estimates are in
329 good agreement with the magnitude of the fitted linear trend both from GRACE and
330 SMB over the period 2003–2014 (van den Broeke et al., 2016) but slightly larger than
331 the reported GRACE-derived mass loss rate from Sutterley et al. (2014), Velicogna et
332 al. (2014) and Forsberg (2017). It should be noted that the overestimation of our
333 results likely comes from the leakage effect of glaciers and ice caps due to the fact
334 that we used extended mascons to fit the GRACE and SMB data. The impact of this
335 part may reach about 20~80 Gt/yr (Bolsch et al. 2013; Velicogna et al., 2013).
336

The Cryosphere Discuss., https://doi.org/10.5194/tc-2018-142
Manuscript under review for journal The Cryosphere
Discussion started: 7 August 2018

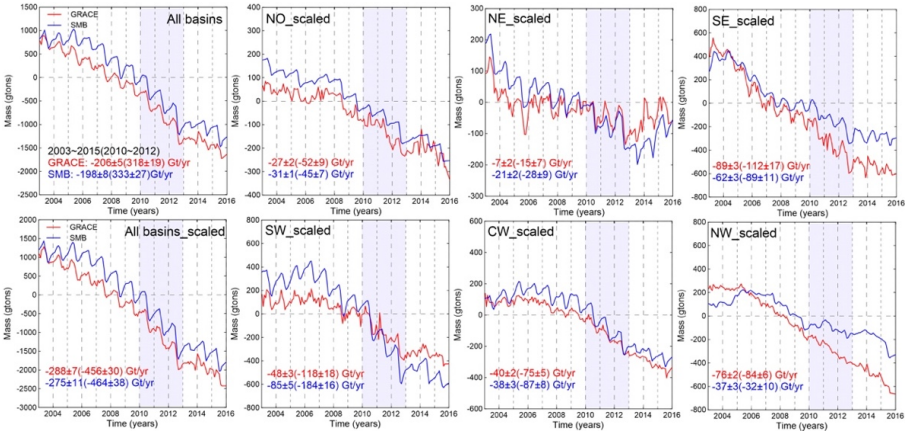

Figure 7. Ice mass change in gigatons (gtons) for GrIS, the top part of the figure from left to right is from the exact mascons of GrIS, extended mascons (after scaled) of NO, NE and SE, respectively. The lower part of the figure from left to right is from the extended mascons (scaled) of GrIS, SW, CW and NW, respectively. GRACE time series for January 2003 to December 2015 (red), time series of cumulative SMB anomaly for January 2003 to December 2015 (blue). Light blue bands represent the time span from January 2010 to December 2012.

For GrIS drainage basins at the regional scale, the melting rate of GrIS in the southern part is significantly higher than in the northern part. The mass loss in the north and northeast was less than –31 Gt/yr for both GRACE and SMB during 2003–2015, and the mass loss of the other four basins (i.e., northwest, central west, south west and southeast) were several times larger than the ones in the two northern regions. The time series of GRACE and SMB revealed that almost all regions experienced large mass losses in 2010–2012. In the southwest and southeast, we found an anomalous acceleration of the mass loss of –118±18 Gt/yr and –112±17 Gt/yr in GRACE and –184±16 Gt/yr and –89±11 Gt/yr in SMB, respectively. The contribution of these two regions is responsible for about 50% of the total loss. In addition, we also found that the melting rate of ice sheets from SMB was greater than the estimates derived from GRACE in the southwest and northeast. This difference indicates that SMB may

The Cryosphere Discuss., https://doi.org/10.5194/tc-2018-142
Manuscript under review for journal The Cryosphere
Discussion started: 7 August 2018

overestimate ice mass changes, since the modeled surface meltwater increases strongly with decreasing elevation and latitude in the low-lying parts of the southwestern GrIS (van den Broeke et al., 2016). In addition, the surface ice elevation was changed by fast-flowing ice dynamics in the southwestern and northeastern areas (Hurkmans et al., 2014). Since 2013, the mass loss slowed down and recovered in the GrIS drainage basins. The agreement between GRACE and SMB results also confirm that the ice sheets returned to near-normal melt conditions, i.e., the refreezing process reduced the melt extent back to normal conditions (Nghiem et al., 2012).

3.3 Sea level fingerprints induced by GrIS

The distribution of GrIS mass changes directly affects the combined contributions of the sea level self-attraction and loading as well as of the ocean-land mass balance resulting in differences in the global sea level distribution (Figure 8). Melting of ice sheets is confirmed over entire Greenland, especially in the southern part and along the coasts (Figure 6). This mass loss of GrIS caused RSL lowering in the entire Arctic Circle, for instance, negative changes of RSL in Scandinavia and Northern Europe up to about –0.6 cm/yr (Figure 8a). It should be noted that the mass loss of Greenland mainly increases RSL in tropical and southern latitudes due to the isostatic rebound of the sea floor around Greenland (Figure 8b).

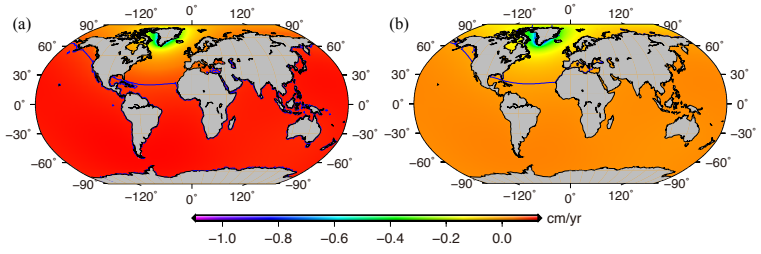

Figure 8. Trends in the sea level fingerprint (SLF) due to mass change of GrIS (a). (b) contributions from the Earth's elastic response. Trends are calculated for the time period January 2003 to December 2015. Blue contour in Figures 8a and 8b is the mean RSL or barystatic sea level equivalent.

Due to ice sheet melting, the sea level along coastlines located up to 2000 kilometers away falls as a result of the isostatic uplift of the crust. The escaping seawater flows across the equator, i.e., the melting of Greenland impacts the coastline of Brazil and the melting of Antarctica affects the United States. These regional differences are significant if we consider the global melting of ice sheets, glaciers and ice caps. For instance, the amount of ice mass melt in the northern hemisphere is higher than in the southern hemisphere, resulting in apparent RSL rise in the South America, South Africa, and Australia, what is nearly 30% higher than the global mean sea level rise rate (Mitrovica et al., 2001; Bamber et al., 2009). In addition, induced by the mass loss of GrIS, the mean RSL trend is approximately 0.07 cm/yr extending through Alaska, Mexico and northern Africa (solid blue line in Figure 8). This pattern illustrates that the dynamic sea level change is determined by the ocean-land mass redistribution and by the instantaneous elastic response of the lithosphere.

4 Discussions

4.1 Sensitivity kernels and rescaling

As an example of the averaging kernel, Figure 9 shows the sum of the sensitivity kernels for all exact and extended mascons shown in Figure 3. Ideally, the solution for mascon fitting would recover the true spatial average of the mascons' mass. When mascons are fitted for the exact-defined GrIS drainage sub-areas (Fig. 3a), the results are automatically scaled. The effective scaling factor based on the least squares mascon approach is defined assuming that surface masses are spread uniformly across any mascon. This method will give exactly the right total mass for that mascon, and will give 0 for the other mascons. However, similar to the optimal averaging kernel method, the mascon fitting based on an exact-defined basin mask (i.e., truly six drainage basins) will also cause weakening of the signal or large uncertainty (e.g., leakage and bias). This is especially the case in boundary areas, which largely contribute to the mass loss, because of the finite number of harmonic degrees in the

The Cryosphere Discuss., https://doi.org/10.5194/tc-2018-142
Manuscript under review for journal The Cryosphere
Discussion started: 7 August 2018

398 GRACE solution. Previous studies suggest that an increasing of the number of
399 mascons covering the anomaly might reduce leakage, so that the anomaly is almost
400 constant across each individual mascon (Jacob et al., 2012). However, there are also
401 indications that using more and smaller mascons can lead to the drawback that the
402 inversion relies more on the higher harmonic degrees.
403 For six sub-areas of the extended mascon (Figure 9b), we assessed a potential impact
404 of the non-uniformity over the exact mascons and external mascons. For the leakage
405 effects, we first computed the mascon distribution between sub-regions, and then we
406 obtained the scale factors by fitting the six extended mascons to the corresponding
407 exact mascons (Table 1). To confirm the validity of signal recovery based on this
408 scaling method, we also used two different regional average methods to compare the
409 results. One method represents a data-driven approach, which is able to restore the
410 GRACE signal loss due to filtering independent of the catchment size (Vishwakarma
411 et al., 2016; 2017). Another method implies scaled optimal averaging functions to
412 recover unbiased mass estimates for six basins (Velicogna and Wahr, 2006).
413

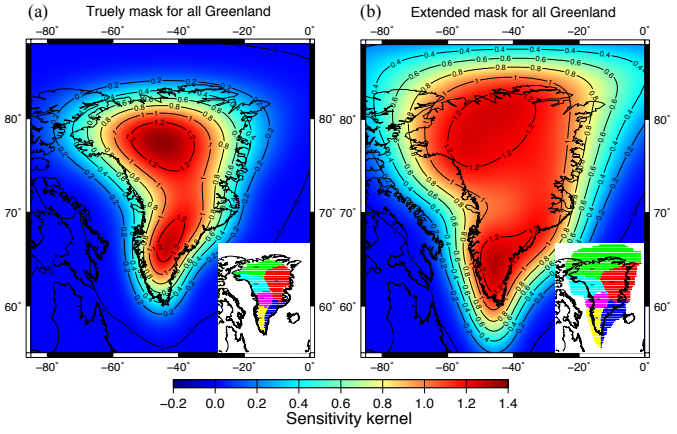

Figure 9. Sensitivity kernel for the truly mask (a) and extended mask (b) of all drainage basins.

414

The Cryosphere Discuss., https://doi.org/10.5194/tc-2018-142
Manuscript under review for journal The Cryosphere
Discussion started: 7 August 2018

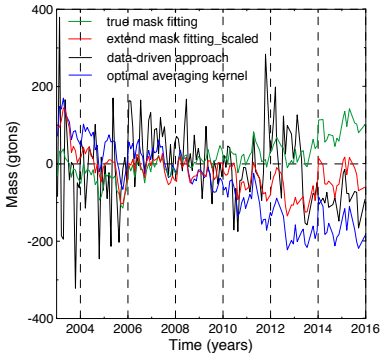

Figure 10. Time series of the true mask fitting mascon and scaled extended mascon fitting in the northeast accompanied by the regional average based on the optimal averaging kernel and data-driven approach.

Exemplarily, Figure 10 shows a validation with the time series comparison between the results from the exact mascon fitting and the extended mascon fitting after rescaling in the northeast. The results confirm that the exact mascon fitting cannot accurately extract the melting contribution of glaciers close to the border (i.e., sensitivity kernel less than 1 shown in Figure 9a). Consequently, the time series from the exact mascon fitting in the northeast show an increasing trend, what is inconsistent with the actual situation and contradicts most previous studies (Velicogna et al., 2014; Sutterley et al., 2014). In addition, the time series obtained by the other two methods also confirm the mass loss trend of ice sheets in the northeast. However, the optimal averaging kernel after scaling may include leakage in other regions and a data-driven approach shows a large noise error in the time series. This is mainly due to the fact that the optimal averaging kernels were created to isolate the gravity signal of individual regions while simultaneously minimizing the effects of GRACE observational errors and contamination from dynamic changes of nearby glaciers (Swenson and Wahr, 2002). Though, this method cannot prevent leakage from adjacent areas. Therefore, there still exists large signal loss in each region due to the filtering and truncation of GRACE coefficients. A data-driven approach was

The Cryosphere Discuss., https://doi.org/10.5194/tc-2018-142
Manuscript under review for journal The Cryosphere
Discussion started: 7 August 2018

433 developed to extract leakage information from the filtered versions of the field, but
434 this method also suffers several limitations, e.g., it does not work with sufficient
435 accuracy for active catchments, and both the scaling factors and the aggregated noise
436 over catchments increase as the catchment size decreases (Vishwakarma et al., 2016).
437
438 **Table 1.** Scale factors of six basins derived with the extended fitting approach

	NO	NE	SE	SW	CW	NW
NO_extended	0.952	0.014	0.000	0.011	−0.005	0.062
NE_extended	0.126	1.063	0.059	−0.031	0.056	0.112
SE_extended	−0.007	−0.021	0.954	0.190	0.071	−0.013
SW_extended	0.012	−0.003	0.071	0.960	−0.098	−0.012
CW_extended	−0.042	0.036	0.151	0.136	1.045	0.050
NW_extended	0.181	0.049	−0.039	−0.033	−0.008	0.964
Ratio of total mass to input mass	1.223	1.138	1.196	1.235	1.061	1.163

439
440 **4.2 Spatial differences of abnormal melting in glacier dynamics**
441 If we ignore the GIA correction error, total mass changes detected by GRACE contain
442 a component caused by changes in SMB (corrected ice discharge) and a component
443 caused by ice dynamics. Usually, the latter can be estimated from satellite altimetry
444 data. Thus, the residuals obtained from GRACE after removing SMB may well reflect
445 glacial dynamics. Figure 11 shows the residuals for each drainage basin and the entire
446 GrIS, which is used to interpret the contribution from glacial dynamics to total ice
447 mass changes. The time series for six drainage basins are quite different and show no
448 overall trend characteristics in GrIS. In the southeast and northwest, there is a
449 negative trend in the difference GRACE minus SMB. Global navigational satellite
450 system data also revealed intense Greenland melting. For example, crustal motion
451 data show that solitary seasonal waves are associated with substantial mass transport
452 through the Rink Glacier in 2010 and 2012 (Adhikari et al., 2017). In contrast, a

The Cryosphere Discuss., https://doi.org/10.5194/tc-2018-142
Manuscript under review for journal The Cryosphere
Discussion started: 7 August 2018

453 positive rate of mass change is found in southwest and northeast areas. In central west,
454 north and entire Greenland, the time series of the residuals do not have apparent
455 trends. This spatial difference is in a good agreement with surface elevation changes
456 derived from ICESat, GRACE and GPS data based on previous results (Howat et al.,
457 2008; Khan et al., 2010; Hurkmans et al., 2014). Particularly, satellite observations
458 such as the Oceansat-2 satellite, MODIS and Special Sensor Microwave
459 Imager/Sounder reveal that melt occurred at or near the surface of GrIS across 98.6%
460 of its surface on 12 July 2012 (Nghiem et al., 2012).
461

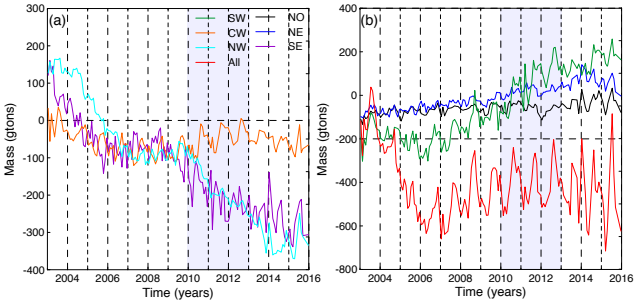

Figure 11. Residuals obtained from GRACE after removing SMB for each drainage basin and the entire GrIS.

462
463 Because of the combination of the modelled (SMB) and observed (GRACE) data, any
464 uncertainty or error of the data source will appear in the residuals. Based on the mass
465 budget method, the SMB model estimates the difference between individual mass
466 sources (mainly snowfall) and sinks (mainly meltwater runoff and solid ice discharge)
467 (van den Broeke et al., 2016). The accumulation/ablation zones of an ice sheet are
468 largely driven by changes in weather conditions (Hanna et al., 2011). More
469 importantly, glacial dynamics refer to the flow of ice from the interior of the ice sheet
470 outward through outlet and land-terminating glaciers (Liu et al., 2016). Although this
471 kind of ice discharge may not be accurately estimated by the SMB model, its
472 contribution to the total mass balance cannot be ignored either. Another factor

473 influencing the residual is the accuracy and limited resolution of GRACE data, e.g.,
474 measurement errors, GIA correction, leakage effects from outside the ice sheet and the
475 eustatic sea level, etc. For Greenland the uncertainties in the GRACE estimates of the
476 ice sheet mass balance have been analyzed in previous studies (Van den Broeke et al.,
477 2009; Bolsch et al. 2013; Velicogna and Wahr, 2013). Therefore, we will not discuss
478 them here in detail. At the same time, we are aware that the errors come mostly from
479 the uncertainty in the scaling factor due to partitioning of GrIS into six mascons. The
480 difference between the non-uniform distribution of actual ice sheets and our
481 assumption of uniform mass distribution within the basin or each mascon also leads to
482 uncertainty of the scaling factor, which increases the uncertainty of final mass loss
483 estimates.

484 **4.3 Near-surface air temperature over the Greenland**

485 In general, mass changes of the GrIS mainly depend on temperature variations, which
486 cause both ice discharge and surface meltwater runoff. Near-surface temperatures can
487 be derived from global land surface models forced with atmospheric data (e.g.,
488 Satellite-derived MODIS data in this study) (Syed et al. 2008). Figure 12 shows the
489 averaged near-surface air temperatures from the GLDAS forcing (i.e, MODIS) data in
490 Greenland for the periods 2003−2015 (Figure 12a) and 2010−2012 after removing
491 the average of 2003−2015 (Figure 12b). The spatial distribution of the temperature
492 anomalies indicates that the increased mass loss rate from GRACE observations and
493 SMB simulations is mainly due to relatively high surface temperature of South
494 Greenland (i.e., mean change range from about −10 to −5 ℃, Figure 5d and Figure
495 6a). According to Figure 12b, there are large positive temperature anomalies over
496 most parts of Greenland during 2010−2012, which is consistent with the acceleration
497 of mass loss in the GrIS during the same period.
498

The Cryosphere Discuss., https://doi.org/10.5194/tc-2018-142
Manuscript under review for journal The Cryosphere
Discussion started: 7 August 2018

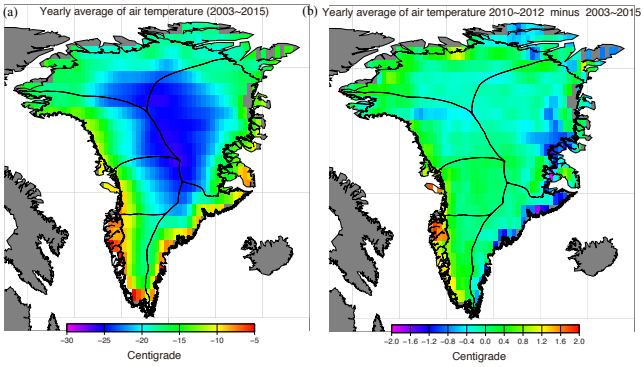

Figure 12. Average near-surface air temperatures from MODIS data in Greenland for the periods 2003−2015 (a) and 2010−2012 after removing the average of 2003 −2015 (b).

499

500 In response to positive near-surface temperature anomalies in the years 2010 and 2012,
501 the GRACE and SMB results show accelerated mass loss (Figure 7). In previous
502 studies, Nghiem et al. (2012) and Hall et al. (2013) already described the major melt
503 event in 2012 in details, which was captured by ice melt maps from three different
504 satellite missions. Seasonal and interannual variations in GRACE time series are
505 qualitatively well reproduced including the large summer mass losses in 2010 and
506 2012 (van den Broeke et al., 2016). In fact, near-surface air temperatures are most
507 appropriate for making long-range predictions of ice melting caused by climate
508 variability. Differences in mass loss between GRACE and SMB are partly attributed
509 to differences in the temperature input of the SMB model. Although not demonstrated
510 in this study, the use of corrected SMB inputs based on in situ data will provide more
511 accurate results when SMB outputs (i.e., sum of mass fluxes towards and away from
512 the surface ice sheets) are used to refine the vertical and horizontal resolutions of
513 GRACE. In turn, this reduces the uncertainty in the GRACE-based estimates of mass
514 changes from ice sheets.

515 **4.4 Contribution of GrIS to sea level change**

516 It is well-known that global mean sea level variations are dominated by thermal

The Cryosphere Discuss., https://doi.org/10.5194/tc-2018-142
Manuscript under review for journal The Cryosphere
Discussion started: 7 August 2018

517 expansion caused by heating of the global ocean, and variations of total ocean mass
518 due to varying water mass fluxes from land to oceans. Here, we attempt to find the
519 contribution of the GrIS to present-day global mean sea level rise. As shown in Figure
520 13, the sum of ocean mass variations from GRACE-derived total land contributions
521 and steric sea level from the total steric sea level anomaly data are close to the
522 observed sea level trend of 3.3 mm/yr derived from sea surface height anomaly data.
523 The trend rate of the contributions of the total land (without Greenland), GrIS and
524 steric sea level changes are 1.1 mm/yr, 0.7 mm/yr and 1.4 mm/yr, respectively.
525

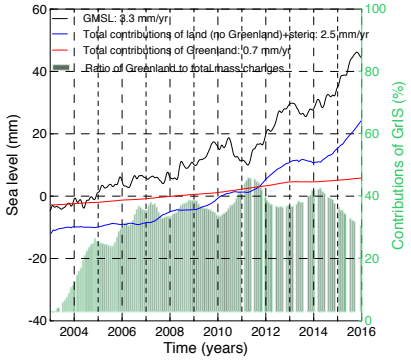

Figure 13. Global mean sea level (GMSL) from altimetry during 2003-2015 (black line), total freshwater input from land (without Greenland) and steric sea level changes (blue line), and GrIS contribution (red line). Seasonal signals have been removed. The grey vertical bars show the contribution rate of GrIS to the total mass change (when GRACE data are available).

526 It is important to note that a V-shaped or solitary wave sea level change is observed
527 from 2010 to 2012 (black line in Figure 13), which is mainly caused by terrestrial
528 water storage anomalies (blue line in Figure 13) related to the 2010/2011 La Niña
529 event (Boening et al., 2012; Fasullo et al., 2013). The GrIS is an important contributor
530 to present-day global mean sea level rise. The average contribution rate (ratio of GrIS
531 to the total mass change) is about 31%. Furthermore, there is a clear acceleration of

the proportion of melting in Greenland (grey vertical bars). It might be stressed that the contribution of GrIS experienced an opposite V-shaped change during 2010-2012, i.e., the sea level changes from rising to falling. This result indicates that increased melting of GrIS partially compensated the sea level drop, which was due to a temporary shift of water from the ocean to continents.

5 Conclusions

In this study, the GrIS variations estimated from GRACE gravity fields and SMB data have been investigated with respect to ice melting of Greenland and its contributions to sea level changes. The spatial pattern of both long-term mass trends obtained from monthly GRACE data and SMB indicates that the ice loss appears clearly over drainage basins in different spatial scales and different time spans. Specifically during the warm period 2010 to 2012, an anomalous acceleration of mass loss occurs in the entire southern and western regions of GrIS, which reflects the major melt event due to higher near-surface temperatures. We calculated time series for six sub-regions defined by mascons using the least squares mascon fitting approach.

We found that the GrIS changes from the extended mascons solutions combined with the matrix scaling factor method are in good agreement with previous studies. The rate of the mass loss obtained by scaled GRACE and SMB is −288±7 Gt/yr and −275±1 Gt/yr, respectively, from 2003 to 2015. The magnitude of this trend increased significantly to −456±30 Gt/yr in GRACE and −464±38 Gt/yr in SMB in the period 2010–2012. The residuals obtained from GRACE after removing SMB may reflect the contribution from glacial dynamics to total ice mass changes. These spatial differences in the residuals among six drainage basins are in good agreement with the surface elevation change rates previously derived from the ICESat data.

We computed SLF due to the ice mass fluxes of Greenland for the time period 2003–2015. RSL anomalies caused by dynamics of the GrIS are not uniformly distributed across the global oceans due to self-attraction and loading effects. Mass loss of the

GrIS induces reduction of RSL at most coasts of Scandinavia and Northern Europe (up to about −0.6 cm/yr), In contrast, RSL rise is concentrated around South America. The contribution ratio of GrIS to total sea level rise increased and the average contribution rate was about 31% from 2003 to 2015. Although the contribution of GrIS has an opposite V-shaped change relative to the sea level changes during 2010−2012, it could not compensate completely the mass transfer from oceans to the continents.

We also assessed a potential impact of the spherical harmonic truncation, spatial averaging of mascon fitting and leakages from other time-dependent signals. The sensitivity kernels for all extended mascons indicate that the sum of kernels is well-localized to their regions and increased the weight of the boundary of GrIS. This study suggests that the rescaled GrIS time series based on a uniform distribution within the basin can effectively reduce the uncertainty caused by non-uniform mass distribution of continental and oceanic areas. However, contributions of leakage effects from outside ice sheets and the eustatic sea level to the total mass errors cannot be avoided when using extended mascons. These factors likely limit the accuracy of the estimated GrIS contributions to sea level changes.

Code and Data availability. The GRACE solutions used in this study are available from CSR (ftp://podaac.jpl.nasa.gov/allData/grace/L2/CSR/RL05/) and the GLDAS/Noah model data is provided by the NASA Goddard Earth Sciences Data and Information Services Center (http://disc.sci.gsfc.nasa.gov/). Prof. Michiel R. van den Broeke for providing RACMO v2.1 and v2.3 SMB fields over Greenland produced by the Institute for Marine and Atmospheric Research (https://www.projects.science.uu.nl/iceclimate/models/). Vishwakarma et al. (2017) for providing the MATLAB implementation of the data-driven approach at: http://www.gis.uni-stuttgart.de/research/projects/DataDrivenCorrection/. The global mean sea level data was downloaded from NASA

588 (https://sealevel.nasa.gov/understanding-sea-level/key-indicators/global-mean-sea-lev
589 el). The total steric sea level anomaly data was downloaded from NOAA
590 (https://www.nodc.noaa.gov/OC5/3M_HEAT_CONTENT/basin_fsl_data.html). We
591 would encourage interested persons to contact the authorship, who are open to
592 providing advice and sharing data and code where possible.
593
594 *Author Contributions.* Linsong Wang conceived the original experiments, performed
595 the main data processing and analysis; Liangjing Zhang helped with the data
596 processing and improve the experiment; Linsong Wang wrote the manuscript;
597 Liangjing Zhang, Chao Chen, Maik Thomas and Mikhail Kaban contributed to the
598 discussion of the results and revising the manuscript.
599
600 *Competing interests.* The authors declare that they have no conflict of interest.
601
602 *Acknowledgments.* We are grateful to Prof. Michiel R. van den Broeke for providing
603 SMB model data. We also thank Dr. Vishwakarma for giving us more help to use the
604 code. This work is supported by the National Natural Science Foundation of China
605 (41504065, 41574070 and 41604060) and the Fundamental Research Funds for the
606 Central Universities, China University of Geosciences (Wuhan).
607
608 **References**
609 A, G. R., Wahr, J. and Zhong, S.: Computations of the viscoelastic response of a 3-D
610 compressible Earth to surface loading: An application to Glacial Isostatic Adjustment
611 in Antarctica and Canada, Geophys. J. Int., 192, 557–572, 2013.
612 Adhikari, S., Ivins, E. R. and Larour, E.: Mass transport wave samplified by intense
613 Greenland melt and detected in solid Earth deformation, Geophys. Res. Lett., 44,
614 4965–497, 2017.
615 Bamber, J. L., Layberry, R. L. and Gogineni, S. P.: A new ice thickness and bed data

set for the Greenland ice sheet: 1. Measurement, data reduction, and errors, J. Geophys. Res. Atmospheres, 106, 33773–33780, 2001.

Bamber, J. L., Riva, R. E., Vermeersen, B. L. and LeBrocq, A. M.: Reassessment of the potential sea-level rise from a collapse of the West Antarctic Ice Sheet, Science, 324, 901–903, 2009.

Beckley, B. D., Callahan, P. S., Hancock, D. W., Mitchum, G. T. and Ray, R. D.: On the "Cal-Mode" Correction to TOPEX Satellite Altimetry and Its Effect on the Global Mean Sea Level Time Series, J. Geophys. Res. Oceans, 122, 8371–8384, 2017.

Boening, C., Willis, J. K., Landerer, F. W., Nerem, R. S. and Fasullo, J.: The 2011 La Niña: So strong, the oceans fell, Geophys. Res. Lett., 39, L19602, 2012.

Bolch, T., Sandberg Sørensen, L., Simonsen, S. B., Mölg, N., Machguth, H., Rastner, P. and Paul, F.: Mass loss of Greenland's glaciers and ice caps 2003–2008 revealed from ICESat laser altimetry data, Geophys. Res. Lett., 40, 875–881, 2013.

Box, J. E., Fettweis, X., Stroeve, J. C., Tedesco, M., Hall, D. K. and Steffen K.: Greenland ice sheet albedo feedback: Thermody-namics and atmospheric drivers, The Cryosphere, 6, 593–634, 2012.

Cheng, M., Tapley, B. D. and Ries, J. C.: Deceleration in the Earth's oblateness, J. Geophys. Res., 118, 740–747, 2013.

Dziewonski, A. M. and Anderson, D. L.: Preliminary reference Earth model, Phys. earth planet. in., 25(4), 297–356, 1981.

Ettema, J., van den Broeke, M. R., van Meijgaard, E., van de Berg, W. J., Bamber, J. L., Box, J. E. and Bales, R. C.: Higher surface mass balance of the Greenland ice sheet revealed by high-resolution climate modeling, J. Geophys. Res., 36, L12501, 2009.

Farrell, W. E.: Deformation of the Earth by surface loads, Rev. Geophys., 10, 761–797, 1972.

Farrell, W. E. and Clark, J. A.: On postglacial sea level, Geophys. J. Int., 46, 647–667, 1976.

644 Fasullo, J. T., Boening, C., Landerer, F. W. and Nerem, R. S.: Australia's unique
645 influence on global sea level in 2010–2011, Geophys. Res. Lett., 40, 4368–4373,
646 2013.
647 Forsberg, R., Sørensen, L. and Simonsen, S.: Greenland and Antarctica ice sheet mass
648 changes and effects on global sea level, Surv. Geophys., 38, 89–104, 2017.
649 Gardner, A. S., Moholdt, G., Cogley, J. G. et al.: A reconciled estimate of glacier
650 contributions to sea level rise: 2003 to 2009, Science, 340, 852–857, 2013.
651 Hall, D. K., Comiso, J. C., DiGirolamo, N. E., Shuman, C. A., Box, J. E. and Koenig,
652 L. S.: Variability in the surface temperature and melt extent of the Greenland ice sheet
653 from MODIS, Geophys. Res. Lett., 40, 2114–2120, 2013.
654 Hanna, E., Huybrechts, P., Cappelen, J., Steffen, K., Bales, R. C., Burgess, E.,
655 McConnell, J. R., Steffensen, J. P., Van den Broeke, M., Wake, L., Bigg, G., Griffiths,
656 M. and Savas, D.: Greenland Ice Sheet surface mass balance 1870 to 2010 based on
657 Twentieth Century Reanalysis, and links with global climate forcing, J. Geophys. Res.,
658 116, D24121, 2011.
659 Howat, I. M., Smith, B. E., Joughin, I. and Scambos, T. A.: Rates of southeast
660 Greenland ice volume loss from combined ICESat and ASTER observations, Geophys.
661 Res. Lett., 35, L17505, 2008.
662 Hurkmans, R. T. W. L., Bamber, J. L., Davis, C. H., Joughin, I. R., Khvorostovsky, K.
663 S., Smith, B. S. and Schoen, N.: Time-evolving mass loss of the Greenland Ice Sheet
664 from satellite altimetry, The Cryosphere, 8, 1725–1740, 2014.
665 Jacob, T., Wahr, J., Pfeffer, W. T. and Swenson, S.: Recent contributions of glaciers
666 and ice caps to sea level rise, Nature, 482, 514–518, 2012.
667 Jentzsch G.: Earth tides and ocean tidal loading, Tidal phenomena, Springer Berlin
668 Heidelberg, 66: 145-171, 1997.
669 Khan, S. A., Wahr, J., Bevis, M., Velicogna, I. and Kendrick, E.: Spread of ice mass
670 loss into northwest Greenland observed by GRACE and GPS, Geophys. Res. Lett., 37,
671 L06051, 2010.

672 Liu, L., Khan, S. A., van Dam, T., Ma, J. H. Y. and Bevis, M.: Annual variations in
673 GPS-measured vertical displacements near Upernavik Isstrøm (Greenland) and
674 contributions from surface mass loading, J. Geophys. Res. Solid Earth, 122, 677–691,
675 2017.
676 Lythe, M. B. and Vaughan, D. G.: BEDMAP: A new ice thickness and subglacial
677 topographic model of Antarctica, J. Geophys. Res. Solid Earth, 106, 11335–11351,
678 2001.
679 Milne, G. A., Mitrovica, J. X. and Davis, J. L.: Near-field hydro-isostasy: The
680 implementation of a revised sea-level equation, Geophys. J. Int., 139, 464–482, 1999.
681 Mitrovica, J. X., Tamisiea, M. E., Davis, J. L. and Milne, G. A.: Recent mass balance
682 of polar ice sheets inferred from patterns of global sea-level change, Nature, 409,
683 1026–1029, 2001.
684 Nghiem, S. V., Hall, D. K., Mote, T. L., Tedesco, M., Albert, M. R., Keegan, K.,
685 Shuman, C. A., DiGirolamo, N. E. and Neumann, G.: The extreme melt across the
686 Greenland ice sheet in 2012, Geophys. Res. Lett., 39, L20502, 2012.
687 Noël, B., van de Berg, W. J., Machguth, H., Lhermitte, S., Howat, I., Fettweis, X. and
688 Van Den Broeke, M. R.: A daily, 1 km resolution data set of downscaled Greenland
689 ice sheet surface mass balance (1958-2015), The Cryosphere, 10, 2361–2377, 2016.
690 Noël, B., van de Berg, W. J., van Wessem, J. M., et al.: Modelling the climate and
691 surface mass balance of polar ice sheets using RACMO2–Part 1: Greenland (1958–
692 2016), The Cryosphere, 12, 811–831, 2018.
693 Peltier, W. R. and Andrews, J. T.: Glacial-Isostatic Adjustment—I. The Forward
694 Problem, Geophys. J. Int., 46, 605–646, 1976.
695 Rignot, E., Velicogna, I., van den Broeke, M. R., Monaghan, A. and Lenaerts, J.:
696 Acceleration of the contribution of the Greenland and Antarctic ice sheets to sea level
697 rise, Geophys. Res. Lett., 38, L05503, 2011.
698 Rodell, M., Houser, P. R., Jambor, U., Gottschalck, J., Mitchell, K., Meng, C. J.,
699 Arsenault, K., Cosgrove, B., Radakovich, J., Bosilovich, M., et al.: The Global Land

Data Assimilation System, Bull. Am. Meteorol. Soc., 85, 381–394, 2004.

Rodell, M., Velicogna, I. and Famiglietti, J. S.: Satellite-based estimates of groundwater depletion in India, Nature, 460, 999–1002, 2009.

Schrama, E. J., Wouters, B. and Rietbroek, R.: A mascon approach to assess ice sheet and glacier mass balances and their uncertainties from GRACE data, J. Geophys. Res. Solid Earth, 119, 6048–6066, 2014.

Shepherd, A., Ivins, E. R., Geruo, A., et al.: A reconciled estimate of ice-sheet mass balance, Science, 338, 1183–1189, 2012.

Sutterley, T. C., Velicogna, I., Csatho, B., van den Broeke, M., Rezvan-Behbahani, S. and Babonis, G.: Evaluating Greenland glacial isostatic adjustment corrections using GRACE, altimetry and surface mass balance data, Environ. Res. Lett., 9, 014004, 2014.

Swenson, S., Chambers, D. and Wahr, J.: Estimating geocenter variations from a combination of GRACE and ocean model output, J. Geophys. Res., 113, B08410, 2008.

Swenson, S. and Wahr, J.: Methods for inferring regional surface- mass anomalies from Gravity Recovery and Climate Experiment (GRACE) measurements of time-variable gravity, J. Geophys. Res., 107, 2193, 2002.

Syed, T. H., Famiglietti, J. S., Rodell, M., Chen, J. and Wilson, C. R. Analysis of terrestrial water storage changes from GRACE and GLDAS, Water Resour. Res., 44, W02433, 2008.

Tamisiea, M. E., Hill, E. M., Ponte, R. M., Davis, J. L., Velicogna, I. and Vinogradova, N. T.: Impact of self-attraction and loading on the annual cycle in sea level, J. Geophys. Res. Oceans, 115, C07004, 2010.

Tapley, B. D., Bettadpur, S., Ries, J. C., Thompson, P. F and Watkins, M. M.: GRACE measurements of mass variability in the Earth system, Science, 305, 503–505, 2004.

Van Angelen, J. H., Van den Broeke, M. R., Wouters, B. and Lenaerts, J. T. M.: Contemporary (1960–2012) evolution of the climate and surface mass balance of the

728 Greenland ice sheet, Surv. Geophys., 35, 1155–1174, 2014.
729 Van den Broeke, M., Bamber, J., Ettema, J., Rignot, E., Schrama, E., van de Berg, W.
730 J., van Meijgaad, E., Velicogna, I. and Wouters, B.: Partitioning recent Greenland
731 mass loss, Science, 326, 984–986, 2009.
732 Van den Broeke, M. R., Enderlin, E. M., Howat, I. M. and Noël, B. P.: On the recent
733 contribution of the Greenland ice sheet to sea level change, The Cryosphere, 10,
734 1933–1946, 2016.
735 Velicogna, I., Sutterley, T. C. and van den Broeke, M. R.: Regional acceleration in ice
736 mass loss from Greenland and Antarctica using GRACE time-variable gravity data, J.
737 Geophys. Res. Space Physics, 41, 8130–8137, 2014
738 Velicogna, I. and Wahr, J.: Acceleration of Greenland ice mass loss in spring 2004,
739 Nature, 443, 329–331, 2006.
740 Velicogna, I. and Wahr, J. Time-variable gravity observations of ice sheet mass
741 balance: Precision and limitations of the GRACE satellite data, Geophys. Res. Lett.,
742 40, 3055–3063, 2013.
743 Vishwakarma, B. D., Devaraju, B. and Sneeuw, N.: Minimizing the effects of filtering
744 on catchment scale GRACE solutions, Water Resour. Res., 52, 5868–5890, 2016.
745 Vishwakarma, B. D., Horwath, M., Devaraju, B., Groh, A. and Sneeuw, N.: A
746 data-driven approach for repairing the hydrological catchment signal damage due to
747 filtering of GRACE products, Water Resour. Res., 53, 9824–9844, 2017.
748 Zwally, H. J., Li, J., Brenner, A. C., Beckley, M., Cornejo, H. G., DiMarzio, J.,
749 Giovinetto, M. B., Neumann, T. A., Robbins, J., Saba, J. L., Yi, D. H.and Wang, W. L.:
750 Greenland ice sheet mass balance: distribution of increased mass loss with climate
751 warming: 2003–07 versus 1992–2002, J. of Glaciology, 57, 88–102, 2011.